

Optimal Design of Piecewise Linear Companding Transforms for PAPR Reduction in OFDM Systems

Sana Mazahir¹, Shahzad Amin Sheikh²

¹ Department of Electrical Engineering, College of Electrical and Mechanical Engineering,
National University of Sciences and Technology, Rawalpindi, Pakistan
[e-mail: sana75@ee.ceme.edu.pk]

² Department of Electrical Engineering, College of Electrical and Mechanical Engineering,
National University of Sciences and Technology, Rawalpindi, Pakistan
[e-mail: sheikh.shahzadamin@gmail.com]

*Corresponding author: Sana Mazahir

*Received August 31, 2015; revised November 5, 2015; accepted November 29, 2015;
published January 31, 2016*

Abstract

Orthogonal frequency division multiplexing (OFDM) signals suffer from the problem of large peak-to-average power ratio (PAPR) which complicates the design of the analog front-end of the system. Companding is a well-known PAPR reduction technique that reduces the PAPR by transforming the signal amplitude using a deterministic function. In this paper, a novel piecewise linear companding transform is proposed. The design criteria for the proposed transform is developed by investigating the relationships between the compander and decompander's profile and parameters with the system's performance metrics. Using analysis and simulations, we relate the companding parameters with the bit error rate (BER), out-of-band interference (OBI), amount of companding noise, computational complexity and average power. Based on a set of criteria developed thereof, we formulate the design of the proposed transform. The main aim is to preserve the signal's attributes as much as possible for a predetermined amount of PAPR reduction. Simulations are carried out to evaluate and compare the proposed scheme with the existing companding transforms to demonstrate the enhancement in PAPR, BER and OBI performances.

Keywords: OFDM, PAPR reduction, companding transform, companding distortion, non-linear distortion

1. Introduction

Orthogonal frequency division multiplexing (OFDM) has been widely adopted as the technology of choice for high speed wireless communication systems including broadband internet access systems and digital audio/video broadcast systems. It offers the advantages of high spectral efficiency, immunity to the effects of multi-path fading and power efficiency [1]. However, the OFDM signal is constructed by the addition of large number of sub-carriers having random amplitudes and phases. Consequently, the signal assumes a highly fluctuating, noise-like envelope. This implies that it has a large dynamic range. Hence, the signal suffers from non-linear distortion due to the presence of high power amplifier (HPA) at the transmitter's front-end. This leads to degradation in the system's performance by elevating the bit error rate (BER) and out-of-band interference (OBI) level.

The dynamic range of the OFDM signal is typically quantified by its peak-to-average power ratio (PAPR). Several techniques have been presented to reduce the PAPR of OFDM signals [2][3]. Partial transmit sequences (PTS), selective mapping (SLM), tone injection (TI), tone reservation (TR) and active constellation extension (ACE) are some instances of probabilistic techniques [2][3]. PAPR can also be reduced at the expense of non-linear distortion by using iterative clipping and filtering (ICF), peak windowing and companding [2][3].

Companding schemes offer the advantages of low implementation complexity and capability of efficiently trading between PAPR and BER. Therefore, the design of companding transforms has been gaining a lot of interest. Several companding transforms have been presented, including linear transforms [4][5], non-linear transforms [6][7][8][9][10][11][12][13][14] and piecewise linear transforms [15][16]. In most recent researches [6][7][8][10][11][13][14], companders have been designed by modifying the amplitude distribution of the OFDM signal. However, amplitude distribution modification is an indirect design methodology. This means that it does not relate the compander and decompander's profile or parameters with the system's performance metrics, including implementation complexity, output PAPR, error performance and OBI. Rather these properties change as a consequence of the change in the signal's amplitude distribution. It is noteworthy, however, that the amplitude distribution itself is not a measure of the system's performance. In contrast, the design approach used in the piecewise linear transform in [15] has been found to provide control over output PAPR, implementation complexity and the amount of companding distortion. But in [15], the transform has been designed by targeting to minimize the amplitude distortion and computational complexity at the transmitter. The effects of decompanding on channel-induced noise and BER are not taken into account. Moreover, the non-invertible nature of clipping operation and frequency contents of companding noise are not properly understood with reference to the profile of companding function.

Recently, an iterative companding transform and filtering (ICTF) scheme [17] has been proposed in which linear and piecewise linear transforms have been selected due to their low implementation complexity. In [18], authors also exploited the design flexibility of piecewise linear transform in [15] to optimize its PAPR reduction performance using adaptive companding.

Motivated by the preferred application of piecewise linear transforms in companding schemes presented in recent works [17][18], in this paper, we propose a novel piecewise linear transform. The proposed transform is derived by formulating design criteria for the optimization of BER and OBI performances of the companded signal. The design criteria is

developed by studying the relationships between the system's performance metrics and compander's profile and parameters. Using simulations and analysis, we investigate the relationship of compander's profile with error performance, amount of invertible and non-invertible companding distortion, spectral contents of companding noise and implementation complexity. The pre-determined constraints on average power and output PAPR are also simultaneously satisfied. The effect of decompanding on channel-induced noise is also taken into consideration so that the compander/decomparer pair can be designed to optimize the BER. Based on the observations and discussions, we develop a set of rules or guidelines that are used in deriving the proposed transform. Simulation results show that the proposed function outperforms the existing companding transforms in terms of BER, OBI, implementation complexity and scalability for a certain value of desired PAPR. It is also more robust to the changing channel conditions.

The remainder of this article has been organized as follows: In Section 2, general model of an OFDM system is described. In Section 3, we develop general design criteria for the compander design, based on which we propose a new companding scheme in Section 4. Performance evaluation of the proposed transform is presented in Section 5. Finally, conclusion is drawn in Section 6.

2. System Model

Fig. 1 shows the block diagram of a typical OFDM system employing a companding/decomparing transform pair. The oversampled, discrete time, complex envelope of the transmitted OFDM signal is given as follows:

$$x_n = \frac{1}{\sqrt{NL}} \sum_{k=0}^{NL-1} X_k \exp\left(\frac{j2\pi kn}{NL}\right), \quad 0 \leq n \leq NL - 1 \quad (1)$$

where N is the number of sub-carriers. X_k comes from input symbol vector $\mathbf{X} = \left[X_0, X_1, X_2, \dots, X_{\frac{N}{2}-1}, \underbrace{0, \dots, 0}_{\frac{N(L-1)}{2}}, X_{\frac{N}{2}}, \dots, X_{N-1} \right]$, that includes data symbols derived from QAM constellation, pilot symbols and null carriers. L is the oversampling factor.

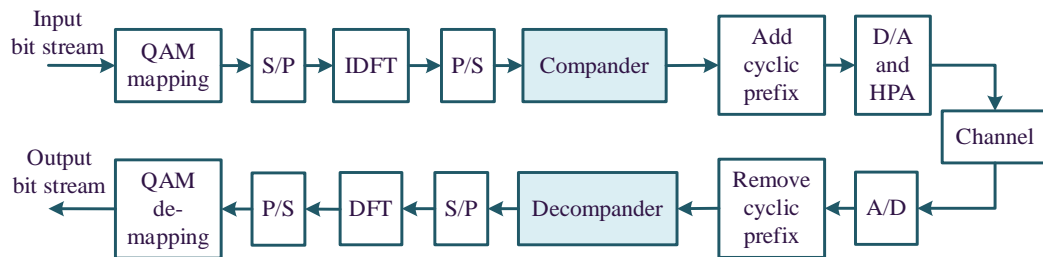


Fig. 1. OFDM system model employing a companding scheme

It is assumed that all the data symbols being added in Eq. (1) are independent and identically distributed (IID). Hence, by central limit theorem (CLT) approximation, OFDM signal is a complex Gaussian random process. The amplitude of a complex Gaussian random process is a Rayleigh process. The probability density function of amplitude $|x_n|$ is given as follows:

$$f_A(x) = \frac{2x}{\sigma_x^2} \exp\left(-\frac{x^2}{\sigma_x^2}\right), \quad x \geq 0 \quad (2)$$

where A is the random variable associated with $|x_n|$, for $0 \leq n \leq NL - 1$, used throughout this text and $\sigma_x^2 = E[|x_n|^2]$.

PAPR of an OFDM symbol is defined as follows:

$$\text{PAPR (dB)} = 10 \log_{10} \left(\frac{\max_{0 \leq n \leq NL-1} |x_n|^2}{\frac{1}{NL} \sum_{n=0}^{NL-1} |x_n|^2} \right) \quad (3)$$

PAPR reduction performance of any scheme is evaluated using the empirical curves of complementary cumulative distribution function (CCDF) of output PAPR [2][3], i.e.,

$$\text{CCDF}_{\text{PAPR}}(\text{PAPR}_0) = \Pr[\text{PAPR} > \text{PAPR}_0] \quad (4)$$

3. General Design Criteria

Companding is a post-modulation operation on OFDM signal amplitude that inevitably introduces non-linear distortion. Consequently, companded signals suffer from elevated BER and OBI as compared to the original signal. The key challenge in the design of companding transforms is to keep this distortion within tolerable limits. In this section, we formulate the design criteria for piecewise linear transforms. Our aim is to design the profile and parameters of the compander such that the non-linear distortion has minimal effect on the system's performance for a given amount of PAPR reduction.

The general form of the companding transform, composed of P linear functions, is given below. It should be noted that the transform only changes the amplitude of the signal while its instantaneous phase remains unaffected.

$$T(x) = \begin{cases} m_1x + c_1, & x \leq a_1 \\ m_2x + c_2, & a_1 < x \leq a_2 \\ \vdots & \\ m_px + c_p, & x > a_{p-1} \end{cases} \quad (5)$$

where $m_1, m_2, \dots, m_p, c_1, c_2, \dots, c_p$ and a_1, a_2, \dots, a_{p-1} are the compander parameters, such that $T(x)$ is a monotonically increasing function.

3.1 Constant Average Power

In companding transformation, it is desired to preserve the average power of the signal so that signal-to-noise ratio (SNR) remains unchanged [2][3]. Hence the parameters $m_1, m_2, \dots, m_p, c_1, c_2, \dots, c_p$ and a_1, a_2, \dots, a_{p-1} must satisfy the following equation:

$$\begin{aligned} \sigma_x^2 &= \int_0^\infty x^2 f_A(x) dx = \int_0^\infty T^2(x) f_A(x) dx = \int_0^{a_1} (m_1x + c_1)^2 f_A(x) dx \\ &+ \int_{a_1}^{a_2} (m_2x + c_2)^2 f_A(x) dx + \dots + \int_{a_{p-1}}^\infty (m_px + c_p)^2 f_A(x) dx \end{aligned} \quad (6)$$

3.2 Hard Clipping for Peak Power Reduction

In the companding operation, peak power of the signal is reduced by compressing larger amplitudes. In order to keep the average power unchanged, the power deficiency due to compression is compensated by expanding the smaller amplitudes. The power deficiency P_D due to compression is expressed as follows:

$$P_D = \int_{x>T(x)} [x^2 - T^2(x)] f_A(x) dx \quad (7)$$

For a desired output PAPR $PAPR_{des}$ and average power σ_x^2 , the maximum amplitude a_m in the companded signal is computed as follows:

$$a_m = \sigma_x 10^{PAPR_{des}/20} \quad (8)$$

If P_D is minimized, then smaller power compensation will be required by expansion. This means that the companding noise, i.e., the difference between transformed and original signals, will also be minimized. In order to achieve $PAPR_{des}$, the companding transform should be such that $T(x) \leq a_m$. Hence,

$$P_D \geq \int_{x>T(x)} [x^2 - a_m^2] f_A(x) dx \quad (9)$$

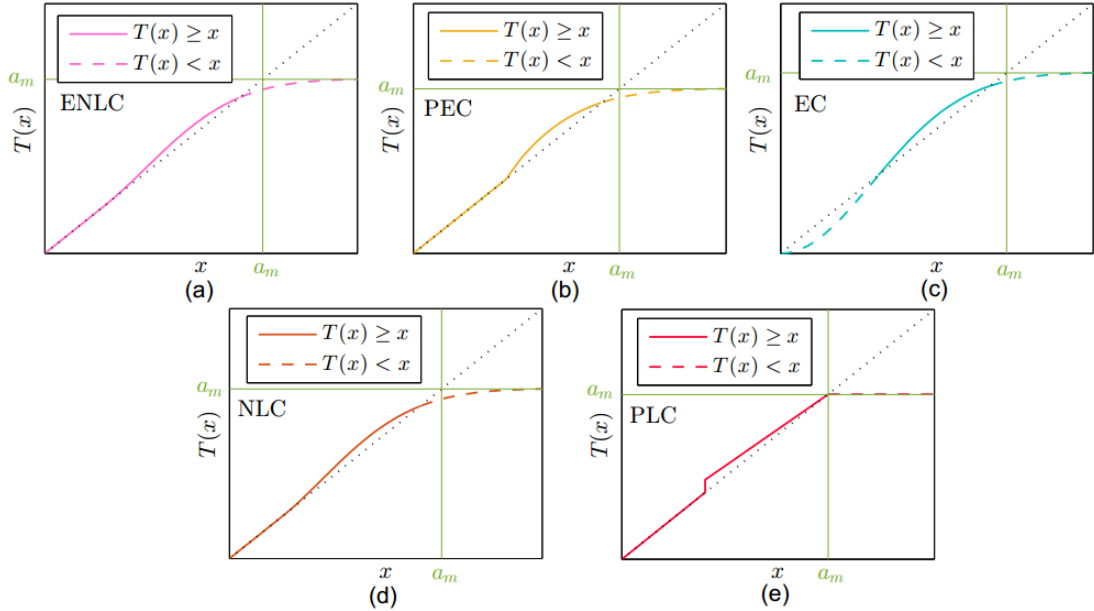


Fig. 2. Profiles of (a) efficient non-linear compander (ENLC) in [8], (b) piecewise exponential compander (PEC) in [9], (c) exponential compander (EC) in [14], (d) non-linear compander (NLC) in [13] and, (e) piecewise linear compander (PLC) in [15]

P_D is going to be minimum when the equality condition in Eq. (9) holds and only the samples with amplitude larger than a_m are compressed.

$$P_{D_{min}} = \int_{x>a_m} [x^2 - a_m^2] f_A(x) dx = \int_{a_m}^{\infty} [x^2 - a_m^2] f_A(x) dx \quad (10)$$

Hence, the transform can be expressed as follows:

$$T(x) = \begin{cases} T_E(x), & x \leq a_m \\ a_m, & x > a_m \end{cases} \quad (11)$$

where $T_E(x)$ represents the expansion transform.

From Eqs. (10) and (11), we infer that hard clipping is the best solution for peak power reduction. This is because it meets the constraint on PAPR without introducing any redundant distortion.

In [6][7][8][9][10][11][12][13][14], companding transforms limit the peak power by soft clipping that results in unnecessary compression. This is illustrated in Figs. 2(a)-(d). We see that soft clipping compresses samples that are already less than a_m and the compressed samples are reduced to levels below a_m , both of which are unnecessary to attain the desired PAPR. In Fig. 2(e), hard clipping is used that does not introduce any redundant compression. Moreover, the compressed part of the signal cannot be recovered without noise amplification (see Sub-section 3.3). Hence, minimizing P_D also ensures that the non-invertible distortion in the signal is minimum.

3.3 Error Performance Optimization

Using the Busgang theorem [19][20], the companded OFDM signal can be represented as the sum of attenuated replica of the original signal and uncorrelated distortion, i.e.,

$$y_n = \alpha x_n + u_n \quad (12)$$

where $y_n = T(|x_n|)\text{sgn}(x_n)$, α is a transform dependent constant and u_n is uncorrelated noise. It is also shown in [19] that α is time invariant and equal to the correlation coefficient of original and companded signals.

$$\alpha = \frac{1}{\sigma_x^2} \int_0^\infty x T(x) f_A(x) dx \quad (13)$$

Now, if $T^{-1}(|x_n|)$ exists, then the decompanded sample r_n can be represented as follows [8][9][10]:

$$r_n = \frac{(x_n + u_n + w_n) - u_n}{\alpha} = x_n + \frac{w_n}{\alpha} \quad (14)$$

where w_n represents additive white Gaussian noise (AWGN) introduced by the channel. Eq. (14) shows that decompanding results in noise amplification by a factor $1/\alpha$. To keep the noise amplification small, α must be as large as possible. It was shown in [8][9][10] that BER decreases with increasing α . Hence the parameters of $T(x)$ must be selected such that correlation coefficient α is maximized while keeping average power unchanged and maximum amplitude equal to a_m . Since correlation coefficient measures the degree of similarity between original and transformed signal, a large value of α ensures that the original signal is preserved to a large extent. This also suggests that the compander's profile should follow the identity transform as closely as possible. Furthermore, the slopes m_1, m_2, \dots, m_p , in Eq. (5), should be either equal to or greater than one [21]. This ensures the respective inverse transforms at the decompander do not cause noise amplification [21].

If $T^{-1}(|x_n|)$ does not exist, as in case of clipped samples, r_n can be represented as follows:

$$r_n = x_n + w_n + c_n \quad (15)$$

where c_n is clipping noise that depends upon $PAPR_{des}$. Clipping noise is minimized if hard clipping is used for compression (see Sub-section 3.2).

According to Eq. (14), the expanded portion of signal can be recovered with tolerable amount of noise amplification. However, the compressed part of the signal cannot be recovered. According to Eq. (15), at low SNR, w_n dominates. This means that the BER will be close to that of the original signal. At high SNR, c_n dominates and the BER approaches a constant value. Since there will always be a minimum amount of noise present in the signal

even at very high SNR, the OFDM systems employing companders have a noise floor. This will be observed in simulation results in Sub-section 5.3. The compander/decompander pair must be designed to keep this noise floor as low as possible. In the proposed transform, this is ensured by employing hard clipping and partial decompanding (Sub-sections 3.2 and 3.5, respectively).

This type of control over the profile of compander is not possible in the amplitude distribution modification method used in previous works [8][9][13][14]. The transform in [15] only considers distortion at the transmitter but the slope of the expansion transform is smaller than 1 (see Fig. 2(e)). Thus even with minimum distortion at the transmitter, noise amplification by the decompander at the receiver is significant.

3.4 Reduction of Out-of-band Interference (OBI) due to Companding Distortion

Since companding is a non-linear operation on the signal, it introduces intermodulation noise. This widens the effective bandwidth of the channel by raising the side-lobe level. It also increases the adjacent channel interference (ACI) due to high frequency contents in the companding noise. The increased side-lobe level and ACI are collectively termed as out-of-band interference (OBI).

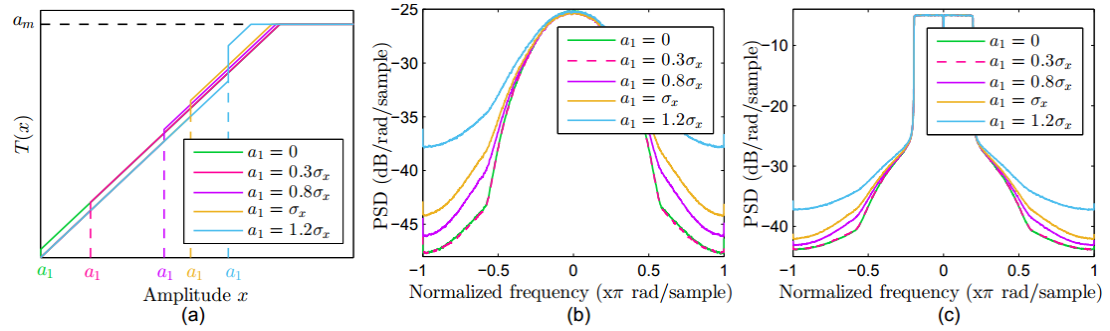


Fig. 3. Relationship between compander's profile and OBI. (a) Companding transforms with changing inflexion points, (b) PSDs of companding noise and, (c) PSDs of companded signals

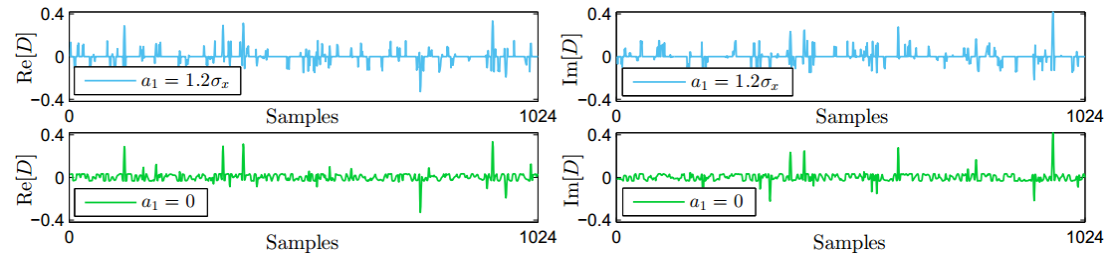


Fig. 4. Waveforms of companding noise, $D = T(x) - x$, for different values of inflexion point a_1

In order to study the relationship between the compander's profile with the amount of OBI, we have used a simple experiment using a transform with one inflexion point:

$$T(x) = \begin{cases} x, & x \leq a_1 \\ x + c_2, & a_1 < x \leq a_m - c_2 \\ a_m, & x > a_m - c_2 \end{cases} \quad (16)$$

where c_2 is the shift introduced in amplitudes greater than the inflexion point a_1 . The transforms for various values of a_1 are shown in **Fig. 3(a)**. It should be noted that each transform satisfies similar constraints on $PAPR_{des}$ and average power. **Figs. 3(b)** and **3(c)** show the power spectral density (PSD) plots of the companding noise, $D = T(x) - x$, and those of the companded signal, respectively. Simulation parameters are given in Sub-section 5.1. It can be observed that as a_1 increases, high frequency contents in the companding noise are also increased. Similar trend is observed in case of OBI in the companded signal.

The observations in **Fig. 3** can be explained by considering the time domain waveform of companding noise. If a_1 is large, then fewer samples will be expanded. Since the expanded signals do not occur consecutively in the time domain waveform, the companding noise comprises of sharp, impulse-like transitions that are added to the original signal. Noise waveforms for a small and a large value of a_1 are shown in **Fig. 4**. We see that when $a_1 = 1.2\sigma_x$, companding noise consists of larger number of sharp transitions and hence more energy at high frequencies. In contrast, for $a_1 = 0$, noise is more uniformly distributed over the time samples. The only sharp transitions are due to the clipping operation which is performed for only a small fraction of samples. As a result, the amplitudes of noise samples are smaller. This means that the waveform of the companded signal will closely follow that of the original signal. Therefore, their spectral contents can also be expected to resemble more closely. Therefore, only a small amount of noise energy leaks into the adjacent channel.

From the observations and discussions, we conclude that OBI will be reduced if the companding noise is well-distributed among all the samples in the signal. Hence we shall select the profile of companding transform in Section 5 such that it expands all the samples with amplitude smaller than a_m , instead of only transforming the larger amplitudes. This is in contrast with the companders in [6][8][9][10][13][14][15] (including the functions in **Fig. 2**) as they only expand the larger samples.

3.5 Partial Decompaning

Since clipping is not invertible, signal can be only partially recovered by the decompander. It should be noted that even in case of soft clipping, compressed part of the signal cannot be recovered without severe noise amplification. In [6][8][12][13][14][17], enhanced performance has been reported if the decompaning operation is eliminated altogether. However, elimination of the inverse operation leads to a heightened noise floor in the system at high SNR. This will be observed in simulation results in Sub-section 5.3. In [15], clipping is also included in the decompander function. But we discovered through simulations that using an identity transform for amplitudes greater than a_m , instead of clipping at the decompander, yields smaller BER. The possible reasons for this observation are:

- The compressed amplitudes in the companded signal are larger than a_m in the original signal. It is possible that the channel-induced noise inadvertently recovers some portions of the clipped peaks.
- Clipping at the decompander changes the frequency contents of the channel-induced white noise. As a result, the amount of the rejected noise, due to the presence of guard band, may be reduced.

Also, since clipping is not invertible, its decompaning counterpart cannot be derived mathematically. Hence, the decompander function has been selected to be as follows:

$$T^{-1}(x) = \begin{cases} T_E^{-1}(x), & x \leq a_m \\ x, & x > a_m \end{cases} \quad (17)$$

Since $T_E(x)$ is going to be designed according to the criteria given in Sub-section 3.3, $T_E^{-1}(x)$ exists for all $x \leq a_m$ and leads to minimal or no noise amplification.

3.6 Scalability

It can be observed that the design criteria has been formulated in such a way that all the performance measures are dealt with for a certain value of $PAPR_{des}$. This means that the compander can be conveniently configured to achieve any PAPR at the output. Also, the parameters of the compander can be simply scaled if transmission power changes. The parameters, that are the cut-off amplitudes and intercepts, $c_1, c_2, \dots, c_p, a_1, a_2, \dots, a_{p-1}$ in Eq. (5), can be obtained for any transmission power by simply multiplying them by σ_x'/σ_x , where $\sigma_x'^2$ is the new transmission power. The slopes, m_1, m_2, \dots, m_p in Eq. (5), are not affected by the change in the required average transmission power. This scalability of parameters can facilitate simpler implementation. The proposed transform is also adequately simple and flexible to be employed in schemes like ICTF [17] and adaptive companding [18].

4. Proposed Compressing Scheme

In this section, we propose a new compressing/decompressing transform pair according to the design criteria developed in Section 3.

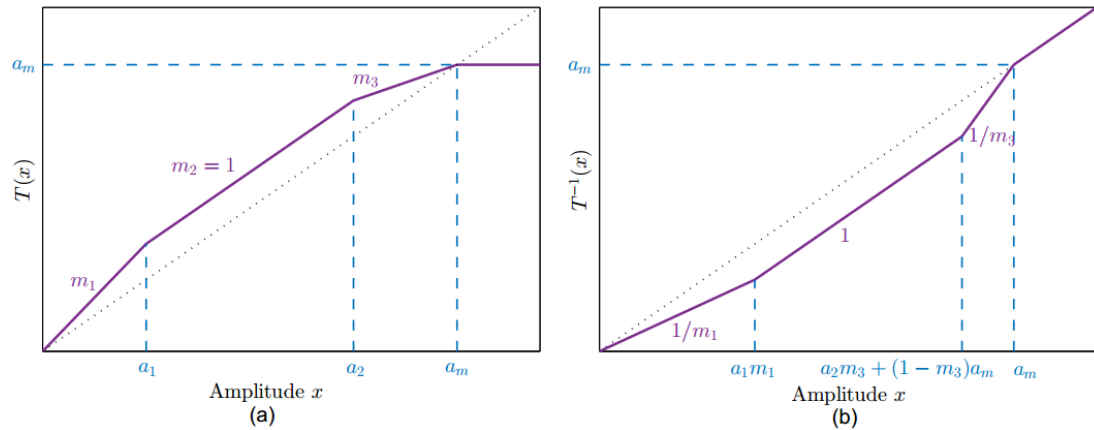


Fig. 5. Profiles of the proposed (a) compressing transform and (b) decompressing transform

4.1 Profiles of the Compressing and Decompressing Transforms

The profiles of the proposed transforms for the compander and decompander are shown in Fig. 5. The proposed compander is composed of four linear functions that are configured by the parameters a_1, a_2, m_1, m_3 and a_m . The compressing transform can be expressed as follows:

$$T(x) = \begin{cases} m_1 x, & x \leq a_1 \\ x + (m_1 - 1)a_1, & a_1 < x \leq a_2 \\ m_3 x + (1 - m_3)a_m, & a_2 < x \leq a_m \\ a_m, & x > a_m \end{cases} \quad (18)$$

According to the discussions and analysis in Sub-section 3.2, hard clipping is used for peak power reduction. To optimize the bit error rate, the slopes are selected such that smaller signals will be amplified to increase SNR, i.e., $m_1 > 1$, the signals with medium amplitudes are expanded without amplification, i.e., $m_2 = 1$, and larger signals are attenuated, i.e., $m_3 < 1$ so that $T_E(x)$ is monotonically increasing and uniquely invertible. Also, all the parameters will be calculated such that the cross-correlation coefficient α is maximized for a given average power and $PAPR_{des}$. As a result, the transform profile closely follows the

identity transform. These specifications are in accordance with our discussions in Sub-section 3.3. Furthermore, following our observations in Sub-section 3.4, the compander's profile is chosen in such a way that the noise due to expansion is well-distributed among all the samples. This is done to keep the OBI level low. This choice slightly increases the computational complexity of the transform but since linear functions already require very few computations and the proposed transform involves larger number of additions than multiplications, the small increase in complexity may be tolerable for most applications.

The decompanding transform is given as follows:

$$T^{-1}(x) = \begin{cases} x/m_1, & x \leq a_1 m_1 \\ x - (m_1 - 1)a_1, & m_1 a_1 < x \leq a_2 m_3 + (1 - m_3)a_m \\ (x - (1 - m_3)a_m)/m_3, & a_2 m_3 + (1 - m_3)a_m < x \leq a_m \\ x, & x > a_m \end{cases} \quad (19)$$

Following the discussion on partial decompanding in Sub-section 3.5, identity transform is used for amplitudes greater than a_m .

4.2 Optimization of the Compander's Parameters

The transform parameters should be such that the average power of the transformed signal remains equal to that of the original signal, i.e.,

$$\sigma_x^2 = \int_0^{a_1} m_1^2 x^2 f_A(x) dx + \int_{a_1}^{a_2} (x + (m_1 - 1)a_1)^2 f_A(x) dx + \int_{a_2}^{a_m} (m_3 x + (1 - m_3)a_m)^2 f_A(x) dx + \int_{a_m}^{\infty} a_m^2 f_A(x) dx \quad (20)$$

Eq. (20) can be expressed as a quadratic equation with respect to m_1 ,

$$b_2 m_1^2 + b_1 m_1 + b_0 = 0 \quad (21)$$

The coefficients b_2, b_1, b_0 are given as follows:

$$b_2 = I_2(0, a_1) + a_1^2 I_0(a_1, a_2) + q^2 I_2(a_2, a_m) + q^2 a_m^2 I_0(a_2, a_m) - 2q^2 a_m^2 I_1(a_2, a_m) \quad (22a)$$

$$b_1 = -2a_1^2 I_0(a_1, a_2) + 2a_1 I_1(a_1, a_2) + 2pq I_2(a_2, a_m) + 2(qr - pq a_m) I_1(a_2, a_m) - q r a_m I_0(a_2, a_m) \quad (22b)$$

$$b_0 = I_2(a_1, a_2) + a_1^2 I_0(a_1, a_2) - 2a_1 I_1(a_1, a_2) + p^2 I_2(a_2, a_m) + r^2 I_0(a_2, a_m) + 2pr I_1(a_2, a_m) + a_m^2 I_0(a_m, \infty) - \sigma_x^2 \quad (22c)$$

where $p = (a_2 - a_1 - a_m)/(a_2 - a_m)$, $q = a_1/(a_2 - a_m)$, $r = a_m - p a_m$, $m_3 = p + q m_1$ and $I_m(a, b) = \int_a^b x^m f_A(x) dx$. a_m is calculated using Eq. (8) according to the value of $PAPR_{des}$.

In order to optimize BER, as discussed in Sub-section 3.3, the parameters a_1, a_2, m_1, m_3 must be such that the correlation co-efficient α is maximized. For the proposed transform, α is given as follows:

$$\alpha = \frac{1}{\sigma_x^2} \int_0^{a_1} x(m_1 x) f_A(x) dx + \frac{1}{\sigma_x^2} \int_{a_1}^{a_2} x(x + (m_1 - 1)a_1) f_A(x) dx + \frac{1}{\sigma_x^2} \int_{a_2}^{a_m} x(m_3 x + (1 - m_3)a_m) f_A(x) dx + \frac{1}{\sigma_x^2} \int_{a_m}^{\infty} x a_m f_A(x) dx \quad (23)$$

$$\alpha = \frac{1}{\sigma_x^2} m_1 I_2(0, a_1) + \frac{1}{\sigma_x^2} I_2(a_1, a_2) + \frac{1}{\sigma_x^2} a_1 (m_1 - 1) I_1(a_1, a_2) + \frac{1}{\sigma_x^2} m_2 I_2(a_2, a_m) + \frac{1}{\sigma_x^2} (1 - m_2) a_m I_1(a_2, a_m) + \frac{1}{\sigma_x^2} a_m I_1(a_m, \infty) \quad (24)$$

Now the compander parameters are obtained by simultaneously solving Eqs. (21) and (24), using **Algorithm 1**. The algorithm first calculates a number of possible solutions of Eq. (21) and then chooses the solution that yields maximum α . **Fig. 6** shows changing values of α with a_2 , for different values of a_1 and $PAPR_{des}$. For each value of a_2 , slope m_3 is also plotted. It can be seen that the α is maximized for a large value of a_2 . The slope m_3 , at the same α is also close to 1, which means that there will be very small amount of noise amplification by the decompanding operation at the receiver.

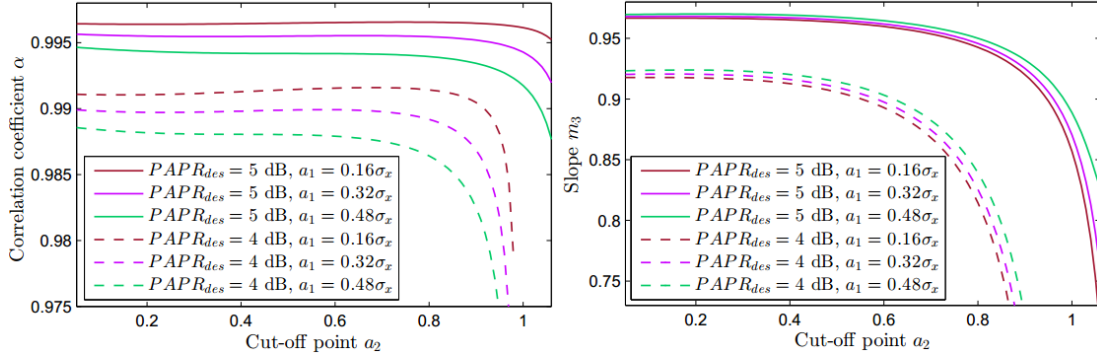


Fig. 6. Relationships between the transform parameters and α

Algorithm 1. Parameters of $T(x)$

- 1) Input $PAPR_{des}$ and σ_x .
 - 2) Initialize solution set $S = \{\}$.
 - 3) Find a_m using Eq. (8).
 - 4) For $a_1 \in (0, a_m)$ and $a_2 \in (a_1, a_m)$, solve Eq. (21) for m_1 . Find $m_3 = p + qm_1$.
 - 5) Add each solution (a_1, a_2, m_1, m_3) , that satisfies the constraints: $m_1 > 1$ and $0 < m_3 < 1$, to the set S .
 - 6) For each element in S , calculate α using Eq. (24).
 - 7) Output parameters (a_1, a_2, m_1, m_3) that maximize α and terminate.
-

5. Performance Evaluation

In this section, we present simulation results for the proposed companding transform. Performance comparison with the companders found in existing researches is also presented. The transforms selected for comparison are efficient non-linear compander (ENLC) in [8], piecewise exponential compander (PEC) in [9], exponential compander (EC) in [14], non-linear compander (NLC) in [13] and piecewise linear compander (PLC) in [15]. Their profiles are shown in **Fig. 2**. The performance evaluation and comparison is done in terms of PAPR reduction performance, error performance, OBI and implementation complexity.

5.1 Simulation Setup and Parameters

OFDM signal is simulated according to the physical layer specifications in IEEE 802.16d used in Fixed Worldwide Interoperability for Microwave Access (WiMAX). Total number of sub-carriers N in an OFDM symbol is 256, including 192 data bearing carriers, 8 pilot carriers and 56 null carriers (guard band and DC). Oversampling factor L is 4. 4- and 16-QAM are used as modulation schemes. Perfect synchronization, ideal channel estimation and zero carrier frequency offset are assumed at the receiver. Stanford university interim (SUI) models given in IEEE 802.16 standard are adopted as multipath channels. Performance with HPA is evaluated using the solid space power amplifier (SSPA) model.

5.2 PAPR Reduction Performance

Fig. 7 shows empirical curves of CCDF of PAPR for original and companded signals. PLC, PEC and ENLC are configured to specific values of output PAPR. The proposed compander is also configured to the same values of PAPR so that the BER and PSDs of the companded signals can be fairly compared. NLC and EC cannot be tuned to any desired PAPR. Their most commonly used configurations are simulated. It can be seen that the proposed compander can be conveniently configured to attain any PAPR at the output.

5.3 Error Performance

Figs. 8-13 show error performance evaluation and comparison of the proposed compander/decompander pair. ENLC, PEC, NLC and EC are simulated without decompanding at the receiver [8][9][13][14]. In case of PLC, both the compander and decompander are simulated [15].

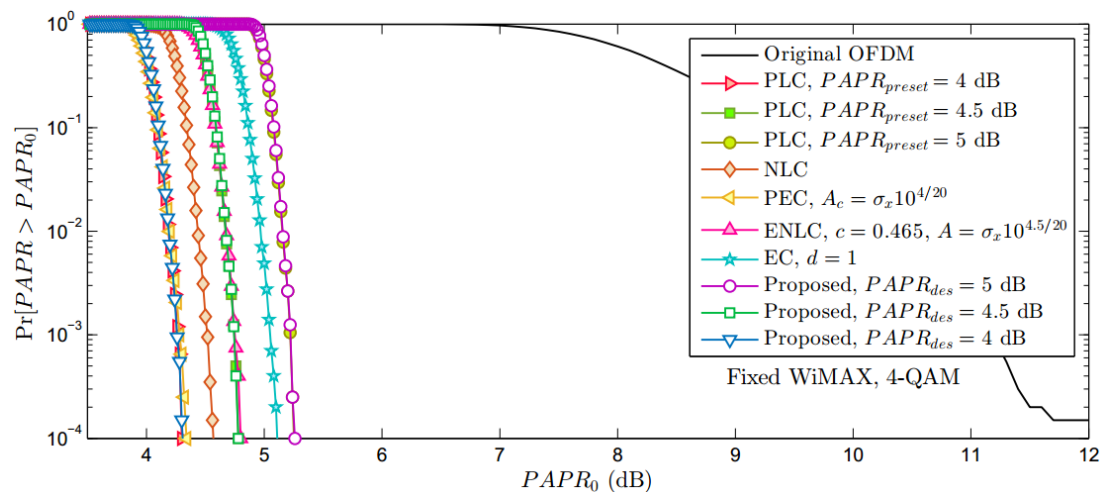


Fig. 7. CCDFs of PAPR of original and companded OFDM signals

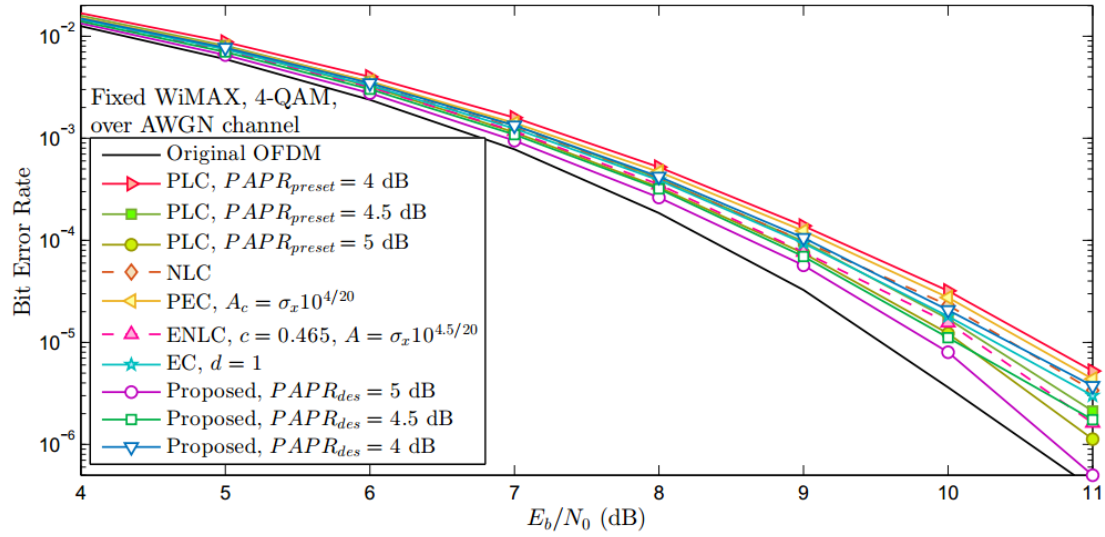


Fig. 8. BER performance comparison of original and companded OFDM signals, over AWGN channel, using 4-QAM modulation

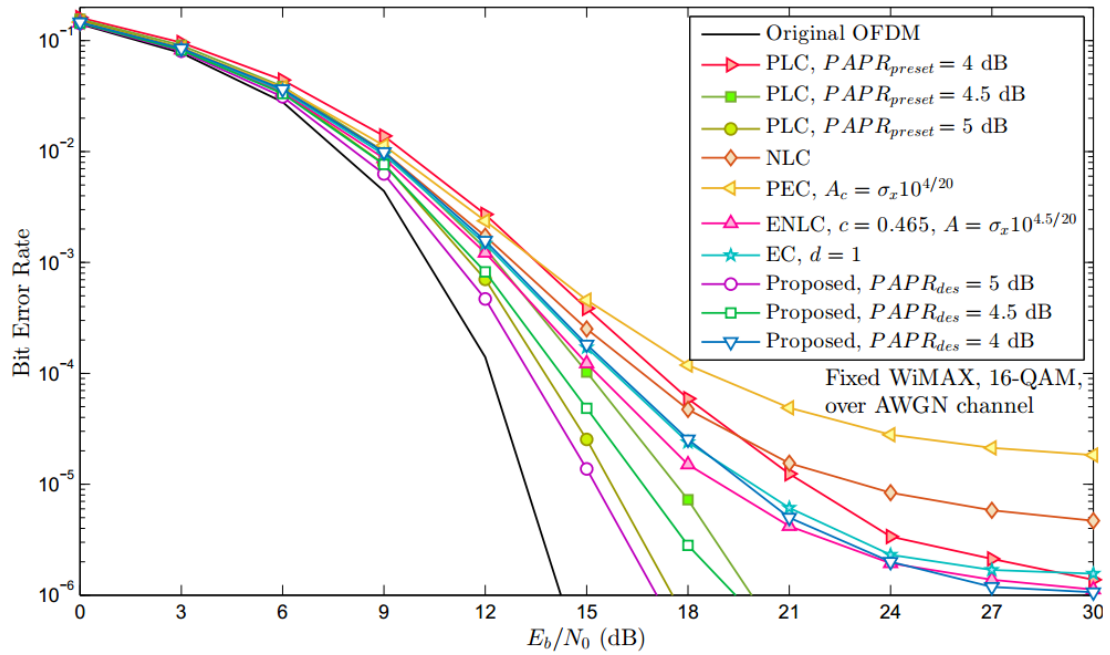


Fig. 9. BER performance comparison of original and companded OFDM signals, over AWGN channel, using 16-QAM modulation

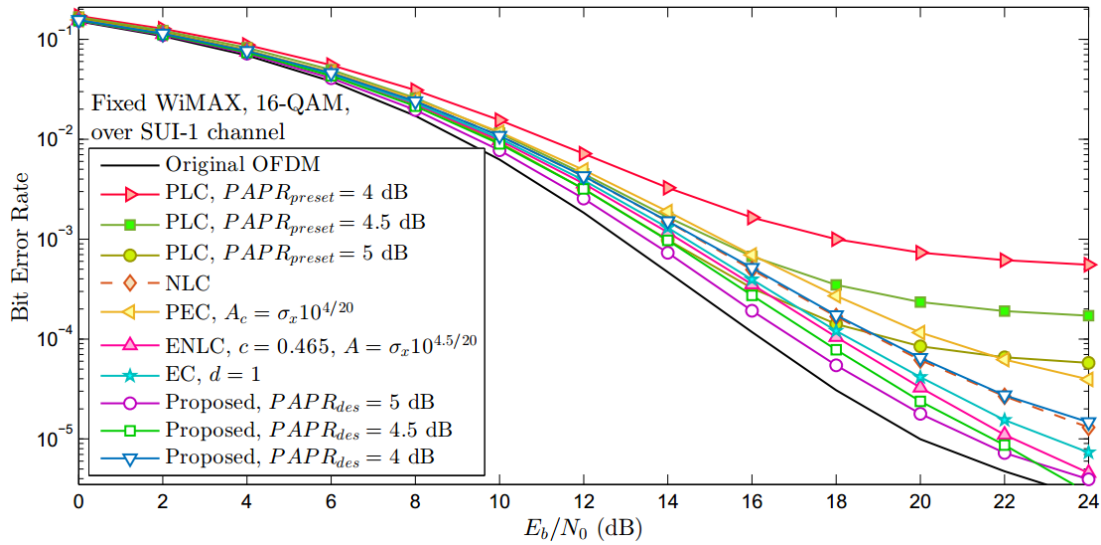


Fig. 10. BER performance comparison of original and companded OFDM signals, over SUI-1 (Rician) channel, using 16-QAM modulation

Evaluation of BER for original and companded signals transmitted over AWGN channel is shown in **Figs. 8** and **9**. It can be seen that the proposed compander can efficiently trade between PAPR and BER, i.e., the error performance gracefully degrades with decreasing $PAPR_{des}$. The proposed transform also outperforms the existing companding schemes. For same PAPR, the proposed transform performs better than PLC, PEC and ENLC. It also performs better than EC and NLC as it yields smaller BER at average PAPR of 4.5 dB as compared to EC at average PAPR of 4.76 dB. Similarly, the proposed scheme gives smaller BER at average PAPR of 4 dB as compared to NLC at average PAPR of 4.25 dB. It can also be observed from **Fig. 9**, that by using partial decompanding and hard clipping in the proposed transform, noise floor of the system at high SNR is considerably lowered as compared to ENLC, NLC, PEC, EC and PLC.

Figs. 10 and **11** show error performance evaluation over multi-path fading channels. We found that generally, the noise amplification due to decompanding has more severe effects in the presence of fading channels and channel estimation. This is due to amplitude scaling of the signal introduced by scattering. In case of SUI-1 (Rician) channel, the proposed compander/decompander pair has been found to outperform all the existing transforms under consideration. It should also be noted that the relative degradation observed for PLC in fading channels as compared to the AWGN channel is due to the fact that its decompander introduces considerable noise amplification at the receiver which is further amplified by channel estimation. The proposed compander/decompander pair performs significantly better than PLC. This is because we have carefully designed both the compander and decompander. It also performs better than ENLC, NLC, EC and PEC that are simulated without decompanding.

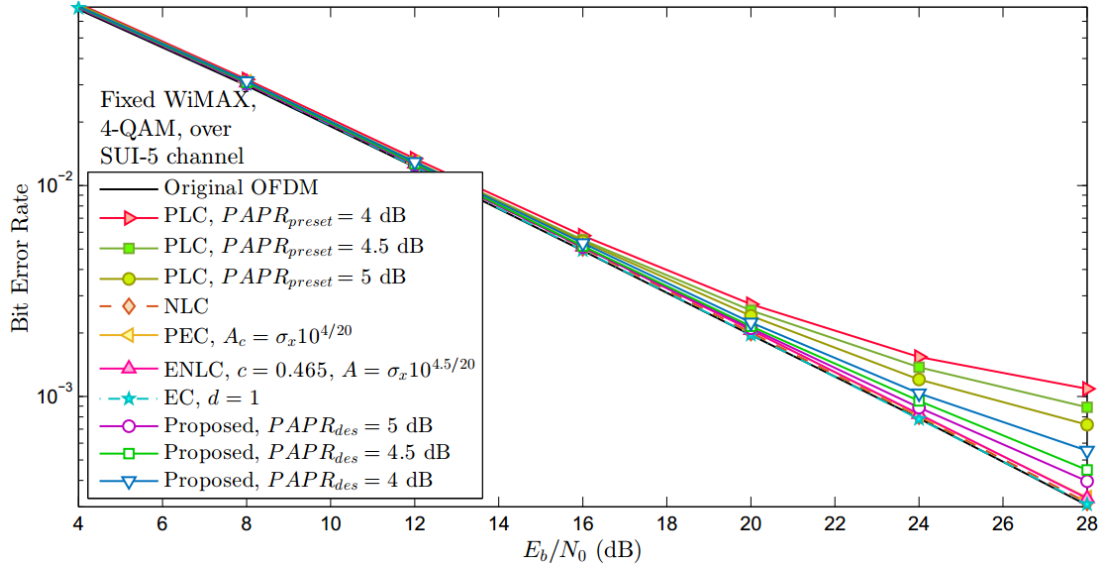


Fig. 11. BER performance comparison of original and companded OFDM signals, over SUI-5 (Rayleigh) channel, using 4-QAM modulation

In case of SUI-5 (Rayleigh) channel, the effects of decompanding are even more severe. We found that without decompanding, all the six companders under consideration yield approximately equal BER, which is equal to the BER of the original OFDM signal. In Fig. 11, it can be observed that the performance of the proposed scheme (with decompanding), at very high E_b/N_0 , slightly degrades as compared to PEC, ENLC, NLC and EC (without decompanding). But it also performs significantly better than PLC (with decompanding) for a wide range of E_b/N_0 . This demonstrates that the performance of the decompander in the proposed scheme has been found to be more enhanced as compared to PLC because it results in a much smaller amount of noise amplification.

When considering the overall performance, shown in Figs. 8-11, we conclude that the proposed scheme performs significantly better than the existing transforms. The proposed scheme is also more robust to the changing channel conditions for a wide range of SNR.

5.4 Performance with HPA

In order to evaluate the performance of companded signals passing through HPA, solid state power amplifier (SSPA) model is used. The input-output characteristics of the SSPA are given as follows [15]:

$$|y(t)| = \frac{|x(t)|}{\left(1 + \left(\frac{|y(t)|}{A_{sat}}\right)^{2p}\right)^{\frac{1}{2p}}} \quad (25)$$

The parameter p determines the extent of non-linearity of the power amplifier near the saturation region. Smaller value of p indicates higher degree of non-linearity. A_{sat} is the saturation level of the amplifier. The efficiency of the amplifier depends on its input back-off (IBO) which must be greater than or equal to the PAPR of the signal [3].

$$\text{IBO (dB)} = P_{sat}(\text{dB}) - P_{avg}(\text{dB}) \quad (26)$$

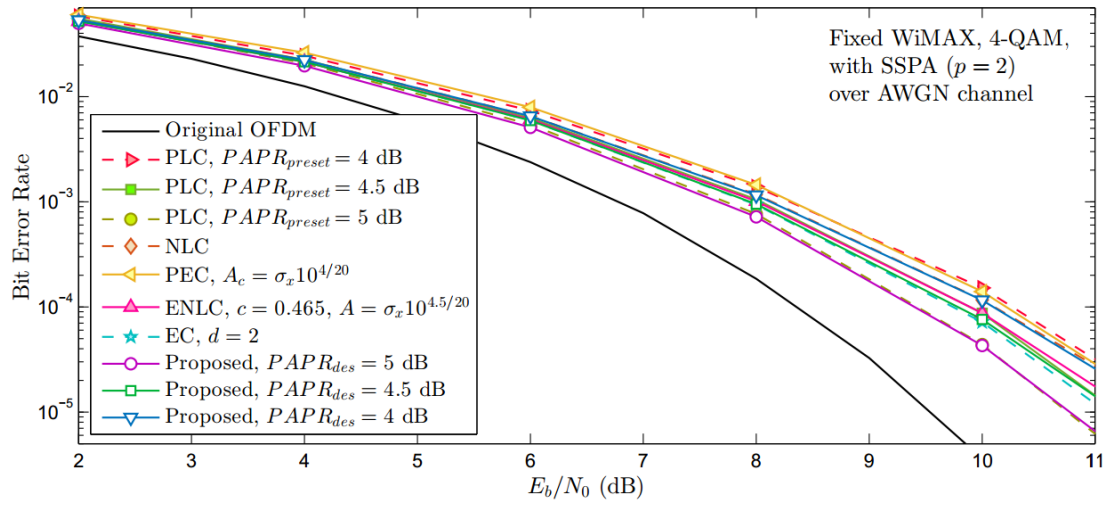


Fig. 12. BER performance comparison of original and companded OFDM signals with SSPA over AWGN channel, using 4-QAM modulation

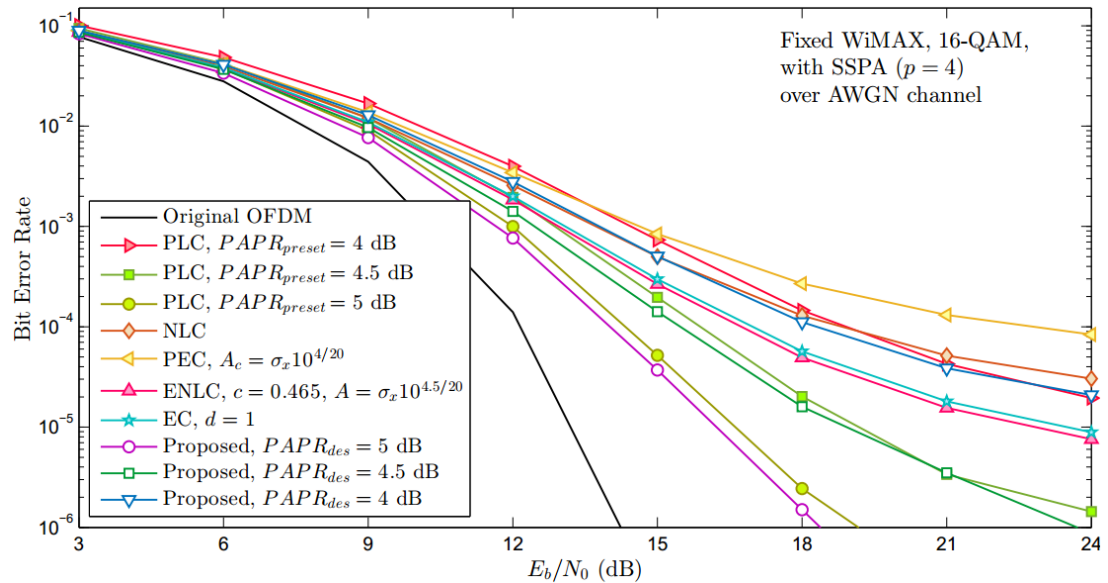


Fig. 13. BER performance comparison of original and companded OFDM signals with SSPA over AWGN channel, using 16-QAM modulation

Using the model in Eq. (25), BER of companded signals passing through SSPA was evaluated over a range of values of p and IBO. **Figs. 12** and **13** show the BER results for two of the cases considered in evaluation. IBO is set to be 0.5 dB higher than average PAPR in each case. We draw following conclusions from this evaluation:

- For highly non-linear HPA (small p), the effect of HPA’s non-linearity has more dominant effect as compared to companding distortion. As a result, all companders at same average PAPR perform almost identically.
- For large p and IBO, the proposed transform surpasses others in performance.

- In the presence of HPA pre-distortion or linearization [22], companded signals will pass through HPA with minimal distortion at $IBO \approx PAPR$. In this case, the proposed transform will surpass the others in performance.

Table 1 summarizes the BER performance comparison. The cases with same average PAPR are highlighted in similar shades so that their performances can be fairly compared.

Table 1. Summary of error performance comparison

Schemes	Mean PAPR (dB)	BER ($\times 10^{-5}$)					
		AWGN		SUI-1	SUI-5	SSPA+AWGN	
		$\frac{E_b}{N_0} =$ 10 dB 4-QAM	$\frac{E_b}{N_0} =$ 15 dB 16-QAM	$\frac{E_b}{N_0} =$ 16 dB 16-QAM	$\frac{E_b}{N_0} =$ 20 dB 4-QAM	$\frac{E_b}{N_0} =$ 10 dB 4-QAM	$\frac{E_b}{N_0} =$ 15 dB 16-QAM
PLC	4	3.200	38.49	164.7	237.7	15.14	73.31
PLC	4.5	1.700	10.28	67.29	255.5	8.75	19.64
PLC	5	1.225	2.538	32.33	240.9	4.388	5.194
NLC	4.25	2.313	25.18	49.49	200.7	11.59	50.39
PEC	4	2.750	45.74	69.46	207.1	13.98	84.06
ENLC	4.5	1.563	12.27	35.22	206.3	8.75	26.63
EC	4.76	1.800	17.13	39.51	195.9	7.15	29.78
Proposed	5	0.800	1.375	19.22	210.6	4.287	3.706
Proposed	4.5	1.112	4.844	27.39	214.9	7.6	14.12
Proposed	4	2.075	18.18	51.52	224.2	11.59	50.39

5.5 Out-of-band Interference (OBI) Level

Fig. 14 shows PSDs of original and companded signals. The PSDs are computed by averaging several periodogram estimates. It can be seen that the proposed transform performs better in terms of side-lobe level and ACI. For same amount of PAPR reduction, the proposed transform results in smaller OBI than ENLC, PEC and PLC. At average PAPR of 4 dB, the ACI using the proposed transform is found to be lower than that with PLC at PAPR of 5 dB, PEC with PAPR of 4 dB, NLC with PAPR of 4.25 dB and EC with PAPR 4.76 dB. At average PAPR of 4.5 dB, ACI with the proposed transform is lower than that in case of ENLC with same PAPR. Side-lobe level, in case of the proposed transform, is also reduced as compared to other transforms for same amount of PAPR reduction. This means that it gives smaller PAPR at lower OBI levels as compared to all the existing transforms under consideration. This is due to the fact that the proposed transform distributes the companding noise among all the samples, thereby limiting the high frequency contents in the companded signal, as discussed in Sub-section 3.4. In contrast, the existing companders only transform higher amplitudes that introduces higher frequency companding noise. **Table 2** summarizes the OBI performance comparison.

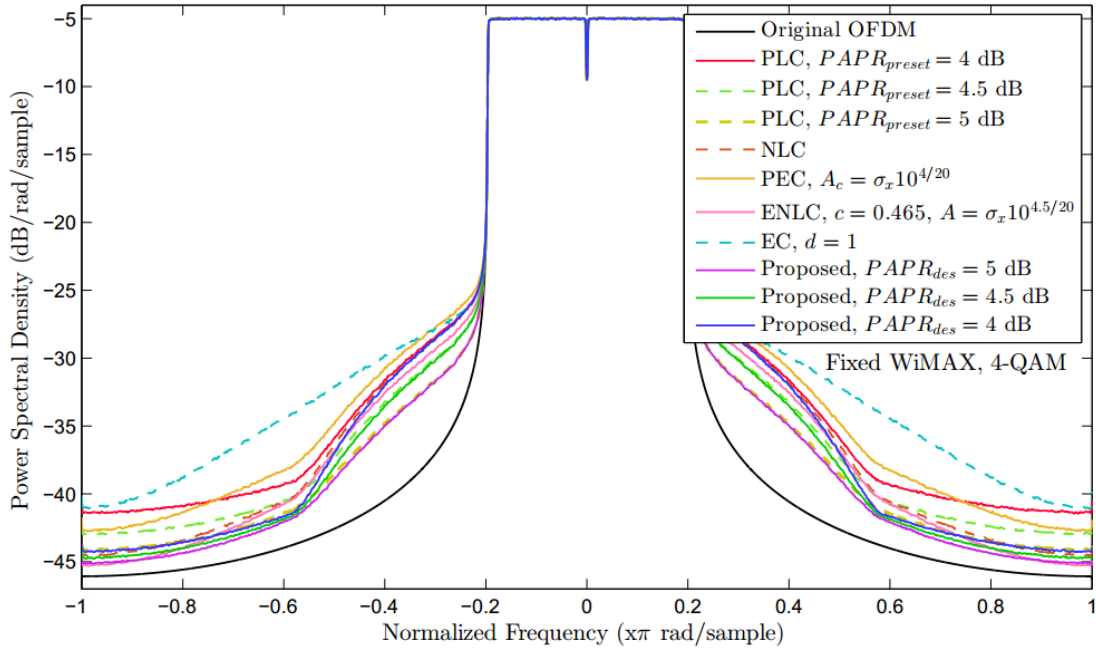


Fig. 14. PSDs of original and companded OFDM signals

Table 2. Summary of OBI performance comparison

Schemes	PLC	PLC	PLC	NLC	PEC	ENLC	EC	Proposed	Proposed	Proposed
Mean PAPR (dB)	4	4.5	5	4.25	4	4.5	4.76	5	4.5	4
Normalized Freq. = 0.4π rad/sample	-31.6	-33.2	-34.8	-31.8	-30.8	-32.5	-29.8	-35.0	-33.5	-32.0
Normalized Freq. = 0.8π rad/sample	-40.9	-42.4	-43.6	-43.4	-41.4	-44.0	-38.8	-44.4	-44.0	-43.7

5.6 Computational Complexity

Piecewise linear transforms are the least complex functions among the companding transforms. This is because they, at most, require only one floating point multiplication and one addition per sample. Computational complexity has been evaluated and compared in terms of MATLAB floating point operations or flops [9][15]. Comparison is shown in Table 3. Since amplitude calculation is common in all cases, only the arithmetic operations in the compander functions are considered. For fair comparison, all the configurable transforms under consideration, namely ENLC, PLC, PEC and the proposed transform, are set to same output PAPR, i.e., 4.5 dB. In cases where decompander is not used, the computations at the receiver can be neglected. Also, it should be noted that although the number of companded samples in the proposed scheme is larger, but for most of the amplitudes, i.e., $NL \int_{a_1}^{a_2} f_A(x) dx$ samples per symbol, only one floating point addition is required.

Table 3. Comparison of computational complexity with existing companding schemes

Schemes	Flops/sample		Number of companded samples (xNL)	Total flops (xNL)
	Transmitter	Receiver		
PLC, $PAPR_{preset} = 4.5$ dB	1	1	$\int_{A_i}^{A_c} f_A(x)dx = 0.596$	1.192
NLC	8	7	$\int_{\sigma_x/\sqrt{6}}^{\infty} f_A(x)dx = 0.85$	12.7
PEC, $A_c = \sigma_x 10^{4.5/20}$	11	9	$\int_{A_i}^{\infty} f_A(x)dx = 0.66$	13.12
ENLC, $A = \sigma_x 10^{4.5/20}, c = 0.465$	35	45	$\int_{c\sigma_x}^{\infty} f_A(x)dx = 0.806$	64.48
EC, $d = 1$	8	7	1	15
Proposed, $PAPR_{des} = 4.5$ dB	1	1	$\int_0^{a_m} f_A(x)dx = 0.94$	1.88

6. Conclusion

In this paper, a novel piecewise linear companding scheme is proposed with the objective of *collectively optimizing* the system's performance in terms of PAPR, BER, OBI and implementation complexity. To achieve this goal, we have conducted experiment/analysis based studies to gain understanding of the relationship of the compander/decompander pair design with several performance aspects. The simulation results show that the proposed transform outperforms the existing ones with regard to BER and OBI for a given PAPR. The simulations over fading channels also suggest that although the proposed scheme demonstrates more robustness to channel conditions as compared to existing ones, but further improvement in error performance can be expected if the effects of channel estimation are incorporated in the decompander design. Enhancement in error performance can also be achieved by integrating clipped signal reconstruction algorithms with the decompander. Hence, more refinements in the decompanding operation at the receiver, especially in the presence of multi-path fading and band limited channel can be considered in future work. Moreover, it was observed that the HPA introduces additional distortion in companded signals. This distortion may be reduced by considering provisions for HPA linearization in the companding transform itself which can reduce the overall complexity of the system.

References

- [1] T. Hwang, C. Yang, G.Wu, and G. Y. Lee, "OFDM and its wireless application: A survey," *IEEE Transactions on Vehicular Technology*, vol. 58, no. 4, pp. 1673-1694, 2009. [Article \(CrossRef Link\)](#)
- [2] T. Jiang and Y. Wu, "An overview: Peak-to-average power ratio reduction techniques for OFDM signals," *IEEE Transactions on Broadcasting*, vol. 54, no. 2, pp. 257-268, 2008. [Article \(CrossRef Link\)](#)
- [3] Y. Rahmatallah and S. Mohan, "Peak-to-average power ratio reduction in OFDM systems: A survey and taxonomy," *IEEE Communications Surveys & Tutorials*, vol. 15, no. 4, pp. 1567-1592, 2013. [Article \(CrossRef Link\)](#)
- [4] S. A. Aburakhia, E. F. Badran, and D. A. E. Mohamed, "Linear companding transform for the reduction of peak-to-average power ratio of OFDM signals," *IEEE Transactions on Broadcasting*, vol. 55, no. 1, pp. 155-160, 2009. [Article \(CrossRef Link\)](#)

- [5] X. Huang, J. Lu, J. Zheng, K. B. Letaief, and J. Gu, "Companding transform for reduction in peak-to-average power of OFDM signals," *IEEE Transactions on Wireless Communications*, vol. 3, no. 6, pp. 2030-2039, 2004. [Article \(CrossRef Link\)](#)
- [6] S. P. DelMarco, "General closed-form family of companders for PAPR reduction in OFDM signals using amplitude distribution modification," *IEEE Transactions on Broadcasting*, vol. 60, no. 1, pp. 102-109, 2014. [Article \(CrossRef Link\)](#)
- [7] Y. Wang, J. Ge, L. Wang, J. Li, and B. Ai, "Nonlinear companding transform for reduction of peak-to-average power ratio in OFDM systems," *IEEE Transactions on Broadcasting*, vol. 59, no. 2, pp. 369-375, 2013. [Article \(CrossRef Link\)](#)
- [8] Y. Wang, L.-H. Wang, J.-H. Ge, and B. Ai, "An efficient nonlinear companding transform for reducing PAPR of OFDM signals," *IEEE Transactions on Broadcasting*, vol. 58, no. 4, pp. 677-684, 2012. [Article \(CrossRef Link\)](#)
- [9] M. Hu, Y. Li, Y. Liu, and H. Zhang, "Parameter-adjustable piecewise exponential companding scheme for peak-to-average power ratio reduction in orthogonal frequency division multiplexing systems," *IET Communications*, vol. 8, no. 4, pp. 530-536, 2014. [Article \(CrossRef Link\)](#)
- [10] S.-S. Jeng and J.-M. Chen, "Efficient PAPR reduction in OFDM systems based on a companding technique with trapezium distribution," *IEEE Transactions on Broadcasting*, vol. 57, no. 2, pp. 291-298, 2011. [Article \(CrossRef Link\)](#)
- [11] J. Hou, J. H. Ge, and J. Li, "Trapezoidal companding scheme for peak-to-average power ratio reduction of OFDM signals," *Electronics Letters*, vol. 45, no. 25, pp. 1349-1351, 2009. [Article \(CrossRef Link\)](#)
- [12] Y. Wang, L. H. Wang, J. H. Ge, and B. Ai, "Nonlinear companding transform technique for reducing PAPR of OFDM signals," *IEEE Transactions on Consumer Electronics*, vol. 58, no. 3, pp. 752-757, 2012. [Article \(CrossRef Link\)](#)
- [13] J. Hou, J. Ge, D. Zhai, and J. Li, "Peak-to-average power ratio reduction of OFDM signals with nonlinear companding scheme," *IEEE Transactions on Broadcasting*, vol. 56, no. 2, pp. 258-262, 2010. [Article \(CrossRef Link\)](#)
- [14] T. Jiang, Y. Yang, and Y.-H. Song, "Exponential companding technique for PAPR reduction in OFDM systems," *IEEE Transactions on Broadcasting*, vol. 51, no. 2, pp. 244-248, 2005. [Article \(CrossRef Link\)](#)
- [15] M. Hu, Y. Li, W. Wang, and H. Zhang, "A piecewise linear companding transform for PAPR reduction of OFDM signals with companding distortion mitigation," *IEEE Transactions on Broadcasting*, vol. 60, no. 3, pp. 532-539, 2014. [Article \(CrossRef Link\)](#)
- [16] P. Yang and A. Hu, "Two-piecewise companding transform for PAPR reduction of OFDM signals," in *Proc. of Wireless Communication and Mobile Computing Conference (IWCMC)*, Istanbul, Turkey, pp. 619-623, 2011. [Article \(CrossRef Link\)](#)
- [17] Y. Wang, C. Yang, and B. Ai, "Iterative companding transform and filtering for reducing PAPR of OFDM signal," *IEEE Transactions on Consumer Electronics*, vol. 61, no. 2, pp. 144-150, 2015. [Article \(CrossRef Link\)](#)
- [18] S. Mazahir and S. A. Sheikh, "An adaptive companding scheme for peak-to-average power ratio reduction in OFDM systems," *KSII Transactions on Internet and Information Systems*, in press.
- [19] P. Banelli and S. Cioffi, "Theoretical analysis and performance of OFDM signals in nonlinear AWGN channels," *IEEE Transactions on Communications*, vol. 48, no. 3, pp. 430-441, 2000. [Article \(CrossRef Link\)](#)
- [20] D. Dardari, V. Tralli, and A. Vaccari, "A theoretical characterization of nonlinear distortion effects in OFDM systems," *IEEE Transactions on Communications*, vol. 48, no. 10, pp. 1755-1764, 2000. [Article \(CrossRef Link\)](#)

- [21] Y. Rahmatallah, N. Bouaynaya, and S. Mohan, "Bit-error-rate performance of companding transforms for OFDM," *IEEE Transactions on Vehicular Technology*, vol. 62, no. 8, pp. 4116–4120, 2013. [Article \(CrossRef Link\)](#)
- [22] B. Ai, Z. Yang, C. Pan, T. Zhang, and J. Ge, "Effects of PAPR reduction on HPA predistortion," *IEEE Transactions on Consumer Electronics*, vol. 51, no. 4, pp. 1143–1147, 2005. [Article \(CrossRef Link\)](#)



Sana Mazahir received the Bachelors in Electrical Engineering from College of Electrical and Mechanical Engineering, National University of Sciences and Technology (NUST), Rawalpindi, Pakistan, in 2013. She recently completed her Masters in Electrical Engineering (DSP and Communications) from NUST. Currently, she is working as Research Assistant in System Analysis and Verification (SAVe) lab at NUST. Her research interests include signal construction and processing for wireless communications, probabilistic analysis and modeling of systems and approximate computing.



Shahzad Amin Sheikh received the B.S. degree in Electrical Engineering from Eastern Mediterranean University (EMU), North Cyprus, in 1995 and Masters in Electrical Engineering from University of New South Wales (UNSW), Sydney, Australia, in 2002. In 2008 he received the Ph.D. from Southwest Jiaotong University (SWJTU), Chengdu, P. R. of China in the field of Information & Communication Systems Engineering. Currently, he is working as a faculty member in Electrical Engineering Department at College of E & ME (a constituent college of National University of Sciences & Technology (NUST), Rawalpindi, Pakistan). His research interests are blind channel equalization and estimation, DSP and its applications in digital communication and biomedical engineering.